Communication

pubs.acs.org/JACS

Isolation of a Terminal Co(III)-Oxo Complex

- ² McKenna K. Goetz, Ethan A. Hill, Alexander S. Filatov, and John S. Anderson*
- 3 Department of Chemistry, University of Chicago, Chicago, Illinois 60637, United States
- 4 Supporting Information

5

6

7

10

11

12

13

14

15

16

17

18

19

20

21

22

23

24

25

26

27

28

ABSTRACT: Late transition metal oxo complexes with high d-electron counts have been implicated as intermediates in a wide variety of important catalytic reactions; however, their reactive nature has often significantly limited their study. While some examples of these species have been isolated and characterized, complexes with d-electron counts >4 are exceedingly rare. Here we report that use of a strongly donating tris(imidazol-2-ylidene)borate scaffold enables the isolation of two highly unusual Co^{III}-oxo complexes which have been thoroughly characterized by a suite of physical techniques including single crystal X-ray diffraction. These complexes display O atom and H atom transfer reactivity and demonstrate that terminal metal oxo complexes with six d-electrons can display strong metal-oxygen bonding and sufficient stability to enable their characterization. The unambiguous assignment of these complexes supports the viability of related species that are frequently invoked, but rarely observed, in the types of catalytic reactions mentioned above. The studies described here change our understanding of the reactivity and bonding in late transition metal oxo complexes and open the door to further study of the properties of this class of elusive and important intermediates.

ransition metal oxo complexes have been proposed as intermediates in a variety of important catalytic reactions. 31 For example, these species have been invoked in biological 32 oxidations such as the degradation of pharmaceuticals by 33 cytochrome P450 enzymes and the formation of oxygen from water during photosynthesis.^{1,2} Metal oxo intermediates are 35 also cited in synthetic systems such as cobalt oxide catalyzed 36 water oxidation and catalytic epoxidations. 3,4 The ubiquity of 37 transition metal oxo complexes in these reactions has 38 motivated synthetic studies to probe their reactivity and 39 plausibility as intermediates. While many examples of terminal 40 oxo complexes have been studied, 5-8 classic bonding theory 41 and experiment suggests that examples with d-electron counts 42 >4 have weakened metal-oxygen bonds making them highly 43 reactive. 9,10 Indeed, only a handful of such species have been 44 reported to date, with many displaying weak metal-oxygen 45 bonding and instability that has limited their character-46 ization. Ĭ1–18

Complexes with six d-electrons are exceptionally difficult to 48 isolate and have been mischaracterized in some cases. 16 A $Re^{\rm I}$ 49 complex utilizing $\pi\text{-accepting}$ acetylene ligands and a $Pt^{\rm IV}$ 50 complex with limited structural information remain the sole 51 examples. 17,18 A strategy which should allow for the isolation

of multiply bonded, high d-electron count complexes is the use 52 of lower coordinate geometries. 19-25 For example, pseudote-53 trahedral geometries can stabilize M-L multiple bonds with 54 late transition metals as evidenced by several examples of M-55 N multiply bonded species. Nevertheless, outside of 56 Wilkinson's d⁴ Ir oxo complex reported 25 years ago, 33 efforts 57 to generate related late transition metal oxo species in 58 pseudotetrahedral ligand environments have proven unsuccessful, as exemplified with tris(pyrazolyl)borate ligands. We 60 rationalized that the stronger carbene donors of the tris-61 (imidazol-2-ylidene)borate ligand PhB(tBuIm)3 recently 62 employed by Smith and co-workers might enable isolation of 63 a d⁶ terminal oxo complex. 12,34

We found that treatment of PhB(^tBuIm)₃Co^{II}Cl with NaOH 65 in THF generates a new species, PhB(^tBuIm)₃Co^{II}OH (1, 66 Scheme 1). Scheme 1). Scheme 1 has been characterized by a suite of 67 s1

Scheme 1. Synthesis of Complexes 1-4

spectroscopic techniques including X-ray diffraction (XRD) 68 that confirm the assignment of a terminal, pseudotetrahedral, *S* 69 = 3/2 Co^{II} hydroxide complex with a Co–O bond length of 70 1.876(2) Å (Figure 1, Figures S1–S6). This bond length is 71 f1 comparable to other pseudotetrahedral Co^{II}-hydroxide com-72 plexes. 36,37 Cyclic voltammetry of 1 in MeCN shows a quasi-73

Received: July 13, 2018 Published: August 5, 2018 Journal of the American Chemical Society

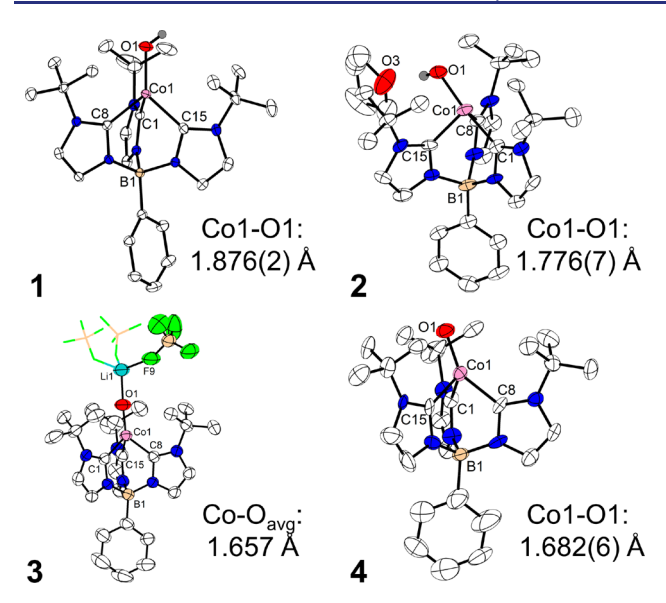


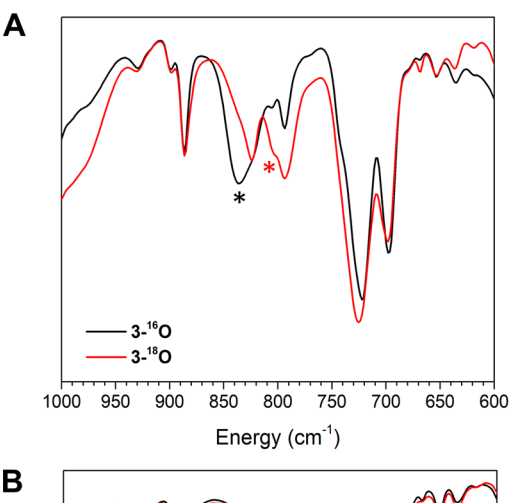
Figure 1. Crystal structures of complexes 1-4. Thermal ellipsoids are shown at 50% probability. All H atoms besides those bound to O are omitted for clarity. Counterions and solvent molecules except for the THF in 2 are also omitted. Only one unit of tetrameric 3 is shown with two of the BF₄ counteranions interacting with the Li⁺ shown in wireframe. The complete structure is shown in Figure S16.

74 reversible couple at -230 mV vs Fc/Fc^+ (Fc = ferrocene) 75 which is assigned to the Co^{II}/Co^{III} redox couple and suggests a 76 Co^{III}-OH species may be chemically accessible (Figure S7). 77 Monitoring the addition of 1 equiv of [Fc][BF₄] to 1 in THF 78 at −78 °C by UV-vis spectroscopy shows an isosbestic 79 conversion from violet 1 to a green species assigned as the one-80 electron oxidized product, [PhB(tBuIm)₃Co^{III}OH][BF₄] (2, 81 Figure S8). This oxidation is also reversible as addition of 82 cobaltocene to in situ generated 2 cleanly regenerates 1 (Figure 83 S9).

While 2 is thermally unstable, it is long-lived enough at 85 temperatures <-35 °C to allow for isolation and character-86 ization. Accordingly, single crystals of 2 were obtained at low 87 temperature and the structure reveals a monomeric Co^{III}-OH 88 complex in a highly distorted, near seesaw geometry. This 89 distorted geometry may be due to a hydrogen bonding 90 interaction with a THF molecule present in the unit cell, but 91 may also have electronic origins. The Co–O bond length in 92 2 has contracted by ~ 0.1 Å from that in 1 to 1.776(7) Å 93 (Figure 1, Table S1), which is comparable to another four-94 coordinate Co^{III}-OH complex.³⁹ Complex 2 is diamagnetic, 95 and its NMR features demonstrate that this complex is C₃ 96 symmetric in solution (Figures S10-S13).

Using 2 as a synthon, we found that treatment with strong 98 bases such as LiHMDS (HMDS = hexamethyldisilazide) 99 results in generation of a new magenta species (3, Figure S14). 100 The reversibility of this reaction by addition of [HNEt₃][BF₄] suggested the new species may be a Co-oxo complex (Figure 102 S15). Analysis of single crystals grown at −35 °C by XRD 103 reveals a tetrameric species with four PhB(^tBuIm)₃Co^{III}O units each capped by a Li⁺ ion and bridged by BF₄⁻ anions to give a 105 monomeric formula of PhB(tBuIm)3CoIIIO·LiBF4 (Figure 1, 106 Figure S16). In this structure, the average Co-O bond length 107 has shortened by an additional ~0.1 Å to 1.657 Å, consistent 108 with deprotonation and an increase in formal bond order. In 109 contrast to 2, the B-Co-O angle is nearly linear at 170.1°. 110 Additionally, isotopically labeled 3 was synthesized from 1-18O

and comparison of the IR spectra of 3-16O and 3-18O shows 111 one isotope dependent feature at 839 cm⁻¹ which shifts to 802 112 cm⁻¹ upon ¹⁸O incorporation, as expected for a simple 113 harmonic oscillator (Figure 2A, Figure S17A). Finally, 3 is 114 f2



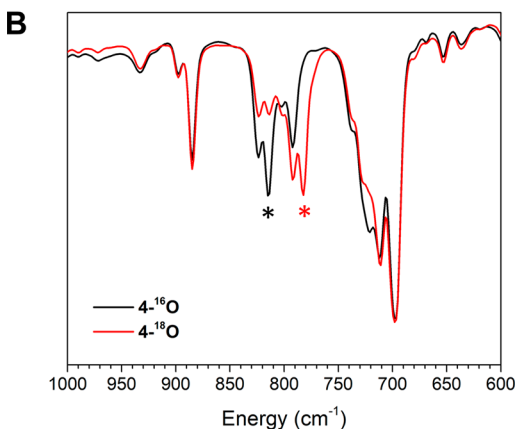
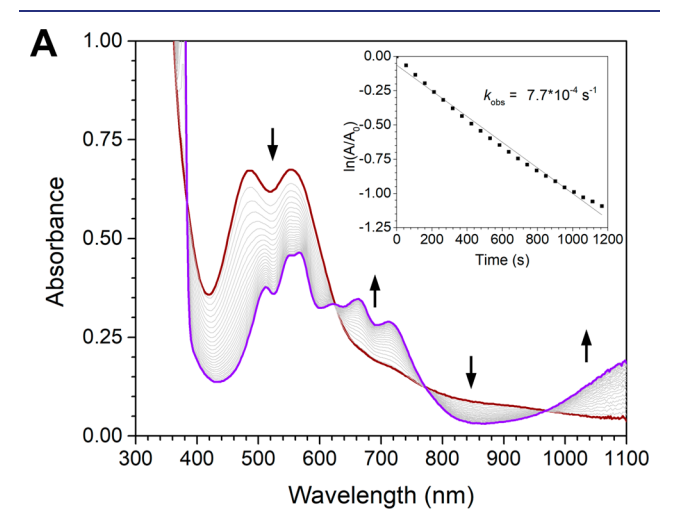


Figure 2. Overlay of IR spectra of ¹⁸O-labeled and natural abundance (A) 3 and (B) 4. Asterisks indicate the feature assigned to the Co-O stretching frequency and its corresponding shift in the ¹⁸O-labeled compound. Difference spectra are shown in Figure S17.

diamagnetic and displays solvent-dependent speciation by 115 NMR spectroscopy in deuterated benzene, THF, and MeCN 116 (Figures S18-S22). This suggested to us that the [Li][BF₄] 117 units in 3 could be separated to isolate a bona fide terminal oxo 118 complex.

Addition of Kryptofix 2,2,1 (4,7,13,16,21-pentaoxa-1,10-120 diazabicyclo [8.8.5] tricosane, crypt) to a benzene solution of 3 121 results in formation of a purple solution of PhB(^tBuIm)₃Co^{III}O 122 (4) and precipitation of $[Li(crypt)][BF_4]$. The successful 123 removal of Li⁺ was confirmed by the loss of signal by ⁷Li NMR 124 spectroscopy. We also note that addition of KHMDS to in situ 125 generated 2 results in formation of 4 directly (see Supporting 126 Information). Furthermore, XRD analysis of single crystals of 4 127 verifies a monomeric complex and shows a Co-O bond length 128 of 1.682(6) Å (Figure 1). There is also a change in the B-Co- 129 O angle upon Li⁺ sequestration from an average of 170.1° in 3 130 to 160.2(3)° in 4 giving a slight but noticeably bent structure 131 in the solid state (Table S1). However, similar to complexes 2 132 and 3, 4 is diamagnetic and its NMR spectra are consistent 133 with a C_3 symmetric species in solution (Figures S23-S25). 134 Finally, IR spectroscopic studies of 4-16O and 4-18O show a 135 feature at 815 cm⁻¹ in the natural abundance complex that 136 137 shifts to 782 cm^{-1} in the ¹⁸O-isotopologue as expected from a 138 simple harmonic oscillator approximation (Figure 2B, Figure 139 S17B). This vibrational frequency is lower than that in 3, 140 consistent with the slightly longer (\sim 0.02 Å) Co-O bond 141 length in 4.^{40,41}

The isolation of these species enabled us to investigate their reactivity with H atom donors and O atom acceptors. While 3 144 and 4 are thermally unstable with solution half-lives of $\sim 6.5-8$ 145 h at room temperature (Table S2), this background reaction is 146 sufficiently slow to allow study of their reactivity with 147 substrates (Figure 3, Figures S26–S27). Both 3 and 4 react



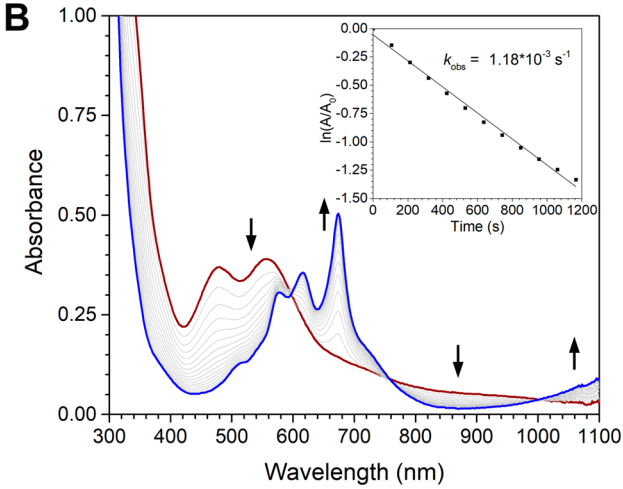


Figure 3. UV—vis spectra of (A) the reaction between 3 (dark red trace) and excess DHA, resulting in formation of 1 (purple trace) and (B) the reaction between 4 (dark red trace) and excess PMe₃ resulting in formation of PhB('BuIm)₃Co^{II}Cl (blue trace). Gray traces indicate 1- and 2-min time intervals, respectively. Insets: first-order kinetic plots of the reaction monitored at 470 nm.

148 with the H atom source DHA (DHA = 9,10-dihydroan-149 thracene) and the O atom acceptor PMe₃ at similar rates 150 (Table S2). Analysis of UV-vis spectra of the reactions with 151 DHA support the formation of anthracene and 1, consistent 152 with net H atom transfer. Similarly, the products of the 153 reactions with PMe₃ are O=PMe₃ from ³¹P NMR spectros-154 copy and what is assigned as PhB(^tBuIm)₃Co^{II}Cl based on 155 previously reported spectral data (Figures S28-S29).³⁵ We 156 speculate that a putative Co^I complex resulting from O atom 157 transfer could react with adventitious chlorine atom sources such as trace dichloromethane (DCM) to give PhB- 158 ([†]BuIm)₃Co^{II}Cl as the major Co-containing product. Attempts 159 to rigorously exclude DCM from the reaction solution lead to 160 formation of O=PMe₃ and 1 as the major Co-containing 161 product (Figure S30), leading us to conclude that the 162 mechanism of this reaction is likely not a simple O atom 163 transfer. Nevertheless, net O atom transfer from Co to P was 164 confirmed by GC-MS analysis of the reaction mixture using 165 ¹⁸O-labeled 3 and 4 (Figure S31).

Having established 4 as a competent H atom abstractor, we 167 sought to estimate the bond dissociation free energy (BDFE) 168 of the O–H bond of 1 using a thermodynamic square scheme 169 (Scheme S1). By taking the $\mathrm{Co^{II}/Co^{III}}$ (1/2) redox potential 170 (see above) and the $\mathrm{p}K_{\mathrm{a}}$ of the $\mathrm{Co^{III}-OH}$ (2), estimated at 171 ~26 in MeCN (Figure S32), a lower bound of 85 kcal/mol for 172 the BDFE of the O–H bond of 1 is obtained. This is 173 consistent with not only the value of 85 kcal/mol predicted by 174 DFT calculations (Table S3) but also the instantaneous 175 reaction between 4 and 2,4,6-tri(tert-butyl)phenol (BDE \approx 82 176 kcal/mol) to produce the corresponding phenoxyl radical and 177 (Figure S33).

Given their unusual nature, the bonding in 3 and 4 merits 179 further discussion. When compared to M-E species with 180 formal triple bonds, 3 and 4 display relatively longer M-E 181 bonds (1.657-1.682(6) Å vs 1.50-1.59 Å) and correspond- 182 ingly lower M-E stretching frequencies (800-850 cm⁻¹ vs 183 950-1000 cm⁻¹). 27,43,44 However, comparison to the sole 184 example of a terminal Co^{IV}-oxo complex with a formal Co-O 185 double bond shows that 3 and 4 have higher Co-O bond 186 orders based on their bond lengths (1.657–1.682(6) Å vs 1.72 187 Å) and vibrational frequencies $(800-850 \text{ cm}^{-1} \text{ vs } 770 \text{ cm}^{-1}).^{15}$ 188 Alternatively, comparison with isoelectronic, pseudotetrahedral 189 Fe^{II}- and Co^{III}-imide complexes shows very similar M-O/-N 190 bond lengths.²⁷ However, direct comparison of the M-E 191 vibrational frequencies is convoluted by mixing of other ligand 192 vibrational modes in the case of the imide complexes. 45 One 193 notable structural difference between 4 and the related imide 194 complexes is the off-axis tilt of the oxo ligand where the B- 195 Co-O angle is 160.2(3)° while the B-Co-N angle in the 196 Co^{III}-imide reported by Smith is 179°.²⁹

To further examine the Co-O interaction in 4 we turned to 198 density functional theory calculations (Figure 4). Analysis of 199 f4 the frontier orbitals reveals two Co–O π^* interactions with d_{xz} 200 and $d_{\nu z}$ parentage as the two highest lying orbitals. These 201 orbitals support the presence of two π -bonds as would be 202 expected for a formal triple bond. The highest occupied orbital 203 in this set is primarily of d_{z^2} parentage and shows a mixed $\sigma^*/204$ nonbonding Co-O interaction. The lowest two orbitals are 205 primarily of d_{xy} and $d_{x^2-y^2}$ parentage and have nonbonding 206 character with respect to the Co-O bond. This orbital picture 207 is analogous to that in related imide complexes suggesting that 208 the bonding in these isoelectronic species is very similar. 209 However, the complex reported here demonstrates an off-axis 210 tilt of the oxo ligand which is not observed in the imide 211 complexes, although computations suggest a relatively low 212 barrier to linearization of ~2 kcal/mol (Table S3). The 213 preference for this bending in the oxo complex is not entirely 214 clear but may likely be attributed to orbital mixing enabled by 215 the weaker ligand field arising from an oxo versus an imide 216 ligand.46

Taken together the results presented here unequivocally 218 validate the assignment of a terminal d⁶ transition metal oxo 219 complex. The computational and experimental analyses are 220

260

2.61

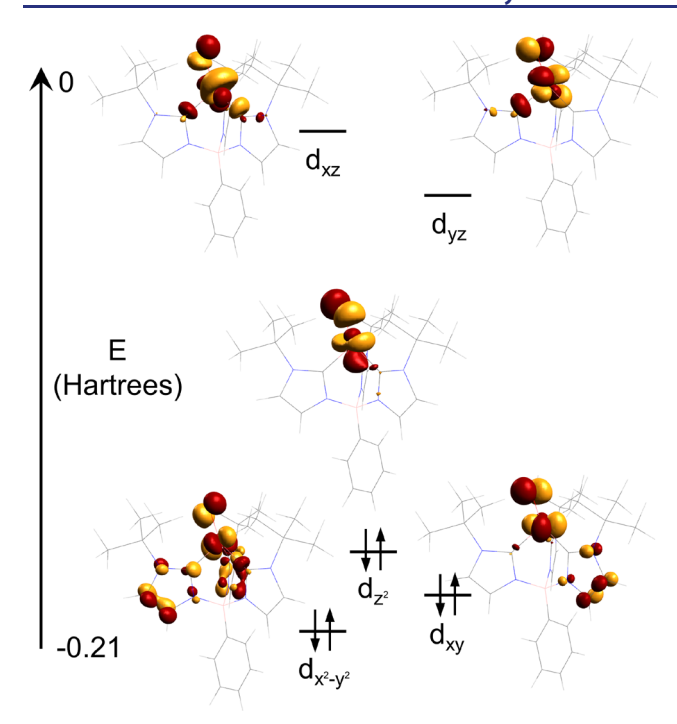


Figure 4. Frontier primarily Co-based molecular orbitals of **4**. The *z*-axis is oriented parallel to the energy axis shown. Note that x and y are arbitrary.

221 consistent with the presence of a strong Co-O interaction 222 with multiple bond character despite a high d-electron count. 223 While the precise nature of this bonding will be an interesting 224 point of discussion and investigation, it is nevertheless clear 225 that these studies provide a concrete example of this unusual 226 class of compounds. The isolation of this complex facilitates 227 further detailed analysis of the properties and reactivity of this 228 and related late transition metal oxo species.

229 ASSOCIATED CONTENT

230 S Supporting Information

The Supporting Information is available free of charge on the ACS Publications website at DOI: 10.1021/jacs.8b07399.

Materials, methods, compound characterization, supplementary figures, schemes, and tables (PDF)

Crystallographic data for CoIIOH and CoIIIOH complexes and Co monomer and tetramer; xyz data for complexes 1 and 4 (ZIP)

238 AUTHOR INFORMATION

239 Corresponding Author

240 *jsanderson@uchicago.edu

241 **ORCID** ®

233

234

242 Alexander S. Filatov: 0000-0002-8378-1994

243 John S. Anderson: 0000-0002-0730-3018

244 Notes

245 The authors declare no competing financial interest.

46 ACKNOWLEDGMENTS

247 ChemMatCARS Sector 15 is principally supported by the 248 Divisions of Chemistry (CHE) and Materials Research 249 (DMR), National Science Foundation (NSF), under Grant 250 No. NSF/CHE1346572. Use of the PILATUS3 X CdTe 1M 251 detector is supported by the National Science Foundation

under Grant Number NSF/DMR-1531283. Use of the 252 Advanced Photon Source, an Office of Science User Facility 253 operated for the U.S. Department of Energy (DOE) Office of 254 Science by Argonne National Laboratory, was supported by 255 the U.S. DOE under Contract No. DEAC02-06CH11357. 256 Work presented here was funded by the following sources: 257 NSF CAREER award Grant No. 1654144, and the University 258 of Chicago.

REFERENCES

- (1) Rittle, J.; Green, M. T. Science 2010, 330, 933-937.
- (2) Cox, N.; Pantazis, D. A.; Neese, F.; Lubitz, W. Acc. Chem. Res. 262 2013, 46 (7), 1588–1596.
- (3) Surendranath, Y.; Kanan, M. W.; Nocera, D. G. *J. Am. Chem. Soc.* 264 **2010**, 132 (46), 16501–16509.
- (4) Lane, B. S.; Burgess, K. Chem. Rev. 2003, 103 (7), 2457-2473. 266
- (5) McDonald, A. R.; Que, L. Coord. Chem. Rev. 2013, 257 (2), 267 414–428.
- (6) Gunay, A.; Theopold, K. H. Chem. Rev. 2010, 110 (2), 1060-269
- (7) Gupta, R.; Taguchi, T.; Lassalle-Kaiser, B.; Bominaar, E. L.; 271 Yano, J.; Hendrich, M. P.; Borovik, A. S. *Proc. Natl. Acad. Sci. U. S. A.* 272 **2015**, 112 (17), 5319–5324.
- (8) Neu, H. M.; Baglia, R. A.; Goldberg, D. P. Acc. Chem. Res. 2015, 274 48 (10), 2754–2764.
- (9) Ballhausen, C. J.; Gray, H. B. Inorg. Chem. 1962, 1 (1), 111–122. 276
- (10) Betley, T. A.; Wu, Q.; Van Voorhis, T.; Nocera, D. G. *Inorg.* 277 *Chem.* **2008**, 47 (6), 1849–1861.
- (11) MacBeth, C. E.; Golombek, A. P.; Young, V. G.; Yang, C.; 279 Kuczera, K.; Hendrich, M. P.; Borovik, A. S. *Science* **2000**, 289 (5481), 280 938–941.
- (12) Smith, J. M.; Mayberry, D. E.; Margarit, C. G.; Sutter, J.; Wang, 282 H.; Meyer, K.; Bontchev, R. P. J. Am. Chem. Soc. **2012**, 134 (15), 283 6516–6519.
- (13) Hong, S.; Pfaff, F. F.; Kwon, E.; Wang, Y.; Seo, M.-S.; Bill, E.; 285 Ray, K.; Nam, W. Angew. Chem., Int. Ed. 2014, 53 (39), 10403–286 10407.
- (14) Matson, E. M.; Park, Y. J.; Fout, A. R. J. Am. Chem. Soc. 2014, 288 136 (50), 17398–17401.
- (15) Wang, B.; Lee, Y. M.; Tcho, W. Y.; Tussupbayev, S.; Kim, S. T.; 290 Kim, Y.; Seo, M. S.; Cho, K. Bin.; Dede, Y.; Keegan, B. C.; Ogura, T.; 291 Kim, S. H.; Ohta, T.; Baik, M. H.; Ray, K.; Shearer, J.; Nam, W. Nat. 292 Commun. 2017, 8, 14839.
- (16) O'Halloran, K. P.; Zhao, C.; Ando, N. S.; Schultz, A. J.; Koetzle, 294 T. F.; Piccoli, P. M. B.; Hedman, B.; Hodgson, K. O.; Bobyr, E.; Kirk, 295 M. L.; Knottenbelt, S.; Depperman, E. C.; Stein, B.; Anderson, T. M.; 296 Cao, R.; Geletii, Y. V.; Hardcastle, K. I.; Musaev, D. G.; Neiwert, W. 297 A.; Fang, X.; Morokuma, K.; Wu, S.; Kögerler, P.; Hill, C. L. *Inorg.* 298 *Chem.* 2012, 51 (13), 7025–7031.
- (17) Spaltenstein, E.; Conry, R. R.; Critchlow, S. C.; Mayer, J. M. J. 300 Am. Chem. Soc. 1989, 111, 8741–8742.
- (18) Poverenov, E.; Efremenko, I.; Frenkel, A. I.; Ben-David, Y.; 302 Shimon, L. J. W.; Leitus, G.; Konstantinovski, L.; Martin, J. M. L.; 303 Milstein, D. *Nature* **2008**, 455 (7216), 1093–1096.
- (19) Mindiola, D. J.; Hillhouse, G. L. J. Am. Chem. Soc. **2001**, 123 305 (19), 4623–4624.
- (20) Dai, X.; Kapoor, P.; Warren, T. H. *J. Am. Chem. Soc.* **2004**, *126* 307 (15), 4798–4799.
- (21) Kogut, E.; Wiencko, H. L.; Zhang, L.; Cordeau, D. E.; Warren, 309 T. H. *J. Am. Chem. Soc.* **2005**, 127 (32), 11248–11249.
- (22) Cowley, R. E.; Holland, P. L. *Inorg. Chem.* **2012**, *51* (15), 311 8352–8361.
- (23) King, E. R.; Sazama, G. T.; Betley, T. A. J. Am. Chem. Soc. 2012, 313 134 (43), 17858–17861.
- (24) Zhang, L.; Liu, Y.; Deng, L. J. Am. Chem. Soc. 2014, 136 (44), 315 15525–15528.
- (25) Wilding, M. J. T.; Iovan, D. A.; Betley, T. A. J. Am. Chem. Soc. 317 **2017**, 139 (34), 12043–12049.

- 319 (26) Liu, Y.; Du, J.; Deng, L. Inorg. Chem. **201**7, 56, 8278–8286.
- 320 (27) Saouma, C. T.; Peters, J. C. Coord. Chem. Rev. **2011**, 255, 920–321 937.
- 322 (28) Jenkins, D. M.; Betley, T. A.; Peters, J. C. J. Am. Chem. Soc.
- 323 **2002**, 124 (38), 11238–11239.
- 324 (29) Cowley, R. E.; Bontchev, R. P.; Sorrell, J.; Sarracino, O.; Feng,
- 325 Y.; Wang, H.; Smith, J. M. J. Am. Chem. Soc. 2007, 129 (9), 2424-326 2425.
- 327 (30) Shay, D. T.; Yap, G. P. A.; Zakharov, L. N.; Rheingold, A. L.;
- 328 Theopold, K. H. Angew. Chem., Int. Ed. 2005, 44 (10), 1508-1510.
- 329 (31) Wu, B.; Hernández Sánchez, R.; Bezpalko, M. W.; Foxman, B. 330 M.; Thomas, C. M. *Inorg. Chem.* **2014**, *53* (19), 10021–10023.
- 331 (32) Hu, X.; Meyer, K. J. Am. Chem. Soc. **2004**, 126 (50), 16322–332 16323.
- 333 (33) Hay-Motherwell, R. S.; Wilkinson, G.; Hussain-Bates, B.;
- 334 Hursthouse, M. B. Polyhedron 1993, 12 (16), 2009-2012.
- 335 (34) Scepaniak, J. J.; Vogel, C. S.; Khusniyarov, M. M.; Heinemann,
- 336 F. W.; Meyer, K.; Smith, J. M. Science 2011, 331 (6020), 1049-1052.
- 337 (35) Cowley, R. E.; Bontchev, R. P.; Duesler, E. N.; Smith, J. M. 338 Inorg. Chem. 2006, 45 (24), 9771-9779.
- 339 (36) Bergquist, C.; Fillebeen, T.; Morlok, M. M.; Parkin, G. J. Am. 340 Chem. Soc. **2003**, 125 (20), 6189–6199.
- 341 (37) Singh, U. P.; Babbar, P.; Tyagi, P.; Weyhermüller, T. *Transition* 342 Met. Chem. **2008**, 33 (8), 931–940.
- 343 (38) Cirera, J.; Ruiz, E.; Alvarez, S. Inorg. Chem. 2008, 47 (7), 344 2871–2889.
- 345 (39) Hana, F.; Lough, A. J.; Lavoie, G. G. Dalt. Trans. 2017, 46, 346 16228–16235.
- 347 (40) Green, M. T. J. Am. Chem. Soc. 2006, 128 (6), 1902-1906.
- 348 (41) Spaeth, A. D.; Gagnon, N. L.; Dhar, D.; Yee, G. M.; Tolman,
- 349 W. B. J. Am. Chem. Soc. 2017, 139 (12), 4477-4485.
- 350 (42) Warren, J. J.; Tronic, T. A.; Mayer, J. M. Chem. Rev. **2010**, 110 351 (12), 6961–7001.
- 352 (43) Evans, J. C. Inorg. Chem. 1963, 2 (2), 372-375.
- 353 (44) Zaragoza, J. P. T.; Siegler, M. A.; Goldberg, D. P. J. Am. Chem. 354 Soc. **2018**, 140 (12), 4380–4390.
- 355 (45) Mehn, M. P.; Brown, S. D.; Jenkins, D. M.; Peters, J. C.; Que, 356 L. *Inorg. Chem.* **2006**, *45* (18), 7417–7427.
- 357 (46) McGarvey, B. R.; Telser, J. Inorg. Chem. **2012**, 51 (11), 6000–358 6010.